ACS OMEGA

Open Access

http://pubs.acs.org/journal/acsodf

Article

Polyoxometalates Mediated Amyloid Fibrillation Dynamics and Restoration of Enzyme Activity of Hen Egg White Lysozyme Treated under Cold Atmospheric Pressure Plasma

Kaberi Kalita, Shankab J. Phukan, Somenath Garai, and Kamatchi Sankaranarayanan*

Cite This: *ACS Omega* 2024, 9, 3423−3429

Read Online

ACCESS | Metrics & More | Article Recommendations

ABSTRACT: Neurodegenerative disorders are one of the most devastating disorders worldwide. Although a definite mechanistic pathway of neurodegenerative disorders is still not clear, it is almost clear that these diseases are initiated by protein misfolding. Hen Egg White Lysozyme (Lyz) can be converted to highly arranged amyloid fibrils and is therefore considered a good model protein for studying protein aggregation in connection to neurodegeneration. In this study, Lyz has been converted to fibrils using He-air gas fed single jet cold atmospheric plasma (CAP). The reactive oxygen species and the reactive nitrogen species produced by the plasma jet interact with the protein molecules and enhance the fibril formation. We monitored the fibrillation kinetics with the Thioflavin T (ThT) assay and observed that fibrils are formed when the samples are treated for 10 min with He-air gas fed CAP. Further, we studied the role of a special class of inorganic nanomaterials called polyoxometalates (POMs) in the process of the Lyz fibrillation using various biophysical techniques. The Keggin POMs used in this study are phosphomolybdic acid (PMA) and silico molybdic acid (SMA). Keggin POMs bring in structural self-assembly of the protein and disrupt the fibrils as evidenced in the ThT assay and TEM analysis. Molecular docking studies together with electrokinetic potential studies show the interactions between POMs and Lyz dominated via hydrogen bonding and electrostatic interactions. The enzyme activity of Lyz was assessed using the substrate *Micrococcus lysodeikticus* and after treatment with POMs results showed a significant increase in the activity. This study could pave way for looking into Keggin POMs for possible application in neurodegeneration.

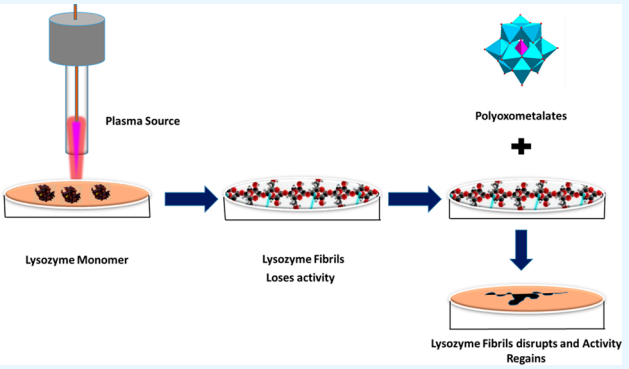

1. INTRODUCTION

Alzheimer's disease (AD) has become one of the most devastating chronic syndromes globally in recent times. Although a definite mechanistic pathway of Alzheimer's disease is still not clear, excruciating research in protein aggregation has confirmed that this disease is initiated by protein misfolding and deposition of the same in the amyloid β structure.[1−3] Amyloid β aggregation is considered to be the main reason responsible for the Alzheimer's diseases.[4] Amyloid β aggregation can be widely categorized into two types, the first being the self-aggregation of naturally occurring amyloid peptide into a cytotoxic oligomeric and fibrillar assembly[5] and the second being amyloid β aggregation by reactive oxygen species (ROS) and reactive nitrogen species (RNS).[6] Amyloid β aggregation can also be induced by the metal ions present in the AD brain, where it is reported that a high concentration of some divalent ions like Zn(II) and Cu(II) interacts with Amyloid β peptide with high affinity.[7] The fundamental reason for almost all the neurodegenerative disorders is the accumulation of the amyloid β fibrils in the brain. Initially, it was thought that only some particular proteins can form amyloid β fibrils and hence can initiate Alzheimer's disease.[8−12] But now it has come to light that any protein can get misfolded and can form amyloid β aggregation and, hence, can initiate Alzheimer's disease.[13] Hen Egg White Lysozyme (Lyz) is considered to be a good model of the AD diseases due to its propensity to form highly ordered amyloid fibrils.[14−16]

Plasma, the fourth state of matter, can be produced in the lab as nonthermal or cold plasma in atmospheric conditions, when a noble gas passes between two electrodes, causing a discharge between the grounded and live electrodes, releasing several reactive species in the medium. In general, plasma is

Received: September 11, 2023
Revised: November 22, 2023
Accepted: November 23, 2023
Published: January 8, 2024

made up of different electrons, ions, neutrals, and reactive oxygen/nitrogen species (RONS)[17−21] and is mainly controlled by the feed gas. In this work, we have used cold atmospheric pressure plasma (CAP) with He-Air as the feed gas to form the fibrils of Lyz utilizing the RONS of CAP and further evaluated the role of a specific class of inorganic nanomaterials against the disruption of these fibrils.

Nanoscience has emerged as one of the fastest growing fields of science in this decade. Its extensive use in medicinal fields in recent times has attracted the eyes of researchers. One of the newly added molecules to the field is polyoxometalates. These astounding groups of molecules are formed by the elements of groups 5 and 6 of the periodic table. The general formula of polyoxometalates is $[(X)_nM_mO_y]^{n-}$ (m > x), where M is the metal ion present and X is any other element in the periodic table. Most of the polyoxometalates are formed by W, Mo, and V.[22−25] POMs with particular structures can inhibit both natural Amyloid β self-aggregation and ROS/RNS induced Amyloid β aggregation.[26−29] POMs particularly with keggin structure have high inhibition property for Amyloid β aggregation.[24] A promising approach toward the development of a novel pharmaceutical agent to treat Alzheimer's disease is to interfere with the amyloid β aggregation and study its interactions with molecules having potential to cure it. However, further investigation is needed to determine whether the protein/enzyme function can be retained and can perform the intended function after the POMs treatment. In this work, we evaluated the activity of lysozyme fibrils after the POMs treatment, using the *Micrococcus lysodeikticus* assay.

In this study, the Lyz has been converted to fibrils using single jet cold atmospheric pressure plasma. As a result, it takes less time to form fibrils with plasma treatment compared to existing methods. Typically, it required low pH and 48−72 h to produce the amyloid fibrils whereas plasma can induce the same within 10 min. The ROS and RNS produced by the plasma jet interact with the protein molecules and enhance the fibril formation. We have evaluated the fibril formation of Lyz using the ThT assay and then studied the role of two different Keggin POMs in the effective inhibition of the amyloid fibrils using various biophysical studies. Finally, utilizing *Micrococcus lysodeikticus* as a substrate, Lyz's enzyme activity was assessed following the treatment with the POMs. This study paves the way for designing POMs as effective inhibitors foramyloid like fibrils.

2. EXPERIMENTAL METHODS

2.1. Materials. Hen Egg White Lysozyme (Lyz) having molecular weight 14 300 kDa was obtained from Sigma (≥99% purity) and was taken at 1 mg/mL concentration for our experiments. All the aqueous solutions used in this study were prepared with a Milli-Q water system (Millipore, type 5, size: 4.7 cm, 0.7 μm retention). The phosphate buffer (pH 7.5, 10 mM) used in this study was prepared by adding monosodium phosphate and disodium phosphate in the required amount. Phosphomolybdic acid (PMA), silicomolybdic acid (SMA), and Thiofavin T were purchased from Sigma-Aldrich, India.

2.2. Plasma Setup. The sample was prepared using a laboratory made single jet Cold Atmospheric Plasma (CAP) device as described in our earlier work[30] with He/Ar/He-air as the feed gas. A quartz tube of 3 mm diameter with a hollow copper/SS electrode of 2 mm diameter was used to produce the plasma. The voltage applied was 4−7 kV with frequency 25 kHz, gas flow rate, and pressure flow of 1 slpm and 1 atm, respectively.Two sets of samples were prepared, one with 8 min of plasma treatment and another with 10 min of plasma treatment. The temperature after the treatment was 30 and 32 °C, respectively. An untreated sample was taken as control. The pH was constant during the whole experiment, at 7.4 before and after the treatment. The entire work was carried out with He-air as the feed gas.

2.3. UV−Visible Spectroscopy. The UV−visible spectroscopic characterization of the samples was analyzed using a Shimadzu UV-Spectrophotometer, model UV-1800.

2.4. Fluorescence Spectroscopy. Cary Eclipse (Varian) fluorescence spectrophotometer was used to study the steady state fluorescence emission of the samples with λ_{ex} = 280 nm and slit width 5 and 10 nm.

2.5. Thioflavin T Assay. To check the formation of protein fibrils have formed, Thioflavin T assay was carried out using a Cary Eclipse (Varian) fluorescence spectrophometer. The fluorescence was recorded with λ_{ex} = 420 nm and slit width 5 and 10 nm.

2.6. Determination of RONS. The levels of various radicals OH, H_2O_2, and Nitrates were determined with assays as mentioned in our earlier work.[31] Hydrogen peroxide was determined using the assay kit from Sigma-Aldrich (Catalog Number MAK165). Hydroxyl radicals were quantified by treating with 20 mM TA and comparing with a standard curve with hydroxyl-terephthalic acid. Nitrate/Nitrite was determined using the detection kit by Cayman Chemicals, USA. All measurements were taken three times, and the average of the same is reported.

2.7. Molecular Docking Study. The crystallographic structure of the lysozyme protein (PDB ID: 1DPX) was obtained from the Protein Data Bank. Subsequently, the lysozyme protein was processed in the Discovery Studio Visualizer by Dassault Systems to remove water and heteroatoms.[31] To facilitate molecular docking studies, PDBQT files for the protein were generated using PyRx software.[32] Additionally, the polyoxometalates (POMs) PMA and SMA underwent energy minimization utilizing the UFF force field with a steepest descent approach consisting of 200 steps. These optimized POM structures were then transformed into AutoDock PDBQT files, again with the assistance of PyRx software. For the molecular docking simulations, the AutoDock Vina program was employed. Each docking run consisted of 10 steps. The population size was set at 300, and a total of 25,000,000 evaluations were performed over 27,000 generations.[33] Finally, to gain insights into the interactions between Lyz and the POMs, the Protein−Ligand Interaction Profiler (PLIP) online tool was utilized for visualization and analysis.

2.8. Zeta Potential Measurements. The Zeta potential was measured by using a ZEN3690 (Malvern). The treated samples (fibrils) without mixing with the POMs were taken as a control. The dispersant medium was water, and the temperature was 25 °C. The equilibrium time was 10 s, and the cell used was a zeta dip cell. Two measurements were taken, and the average of them was used.

2.9. Transmission Electron Microscopy (TEM). For the TEM studies, a TECNAI FE12 TEM instrument, whose operating voltage is 120 kV, was used. The sample was prepared using copper grids (200 mesh size) with carbon coating, and to obtain the images, SIS imaging software was used. No staining agent was used for the TEM analysis. The POMs used for this work were of the concentration 5 mM.

https://doi.org/10.1021/acsomega.3c06921
ACS Omega 2024, 9, 3423−3429

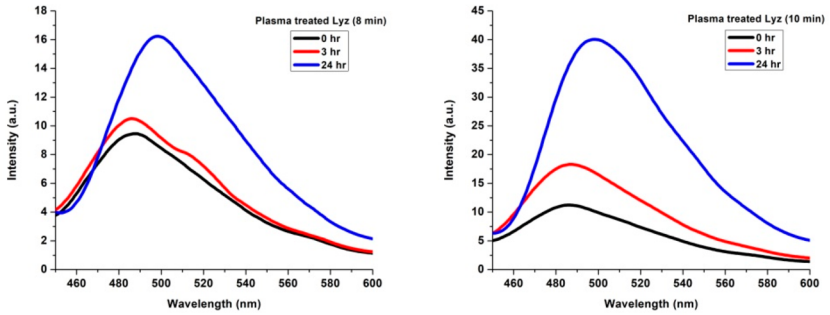

Figure 1. ThT assay of the plasma treated lysozyme for 8 and 10 min (0 h represents the samples immediately after the CAP treatment).

Table 1. Quantification of the Radicals

Plasma treatment time (min)	Hydroxyl radicals (μM)	H_2O_2 (μM)	Nitrate (μM)	Nitrite (μM)
8	55.943 ± 0.088	3.609 ± 0.005	41.950 ± 0.133	8.680 ± 0.081
10	43.363 ± 0.042	3.716 ± 0.006	52.253 ± 0.503	10.760 ± 0.079

2.10. Lysozyme Activity Assay. To confirm whether the POMs used in this study can influence the activity of the POMs treated Lyz fibrils, we performed an assay using *Micrococcus lysodeikticus*, ATCC No. 4698, lyophilized cells (M3770). The assay was performed using a SHIMADZU UV Spectrophotometer, model UV-1800. The absorbance at 450 nm was measured, and the percentage activity was calculated using eq 1:

$$\%\ \text{activity} = (\text{Cell wall suspension} + \text{POM fib solution}) - (\text{Cell wall suspension} + \text{Lyz Monomer}) / (\text{Cell wall suspension} + \text{POM}) \quad (1)$$

The concentration of the cell wall suspension was taken as 0.25 mg/mL. The concentrations of the fibrils and the monomer were kept constant, and the POMs were taken in three concentrations: 1 μM, 100 μM, and 5 mM. All measurements were done in triplicate, and the average was used for the calculation of the percentage activity.

3. RESULTS AND DISCUSSIONS

Lyz protein treated under CAP was evaluated using the standard ThT assay. Additionally, the structure of the Thioflavin T molecule and its preferential binding to amyloid fibrils make it a unique candidate for studies associated with amyloid fibrils. The Lyz samples after the CAP treatment were subjected to a time dependent ThT Assay to confirm fibril formation. Initially the protein solutions were studied with pure Helium and Argon as the feed gas in a CAP jet, with treatment times of 8 and 10 min. However, the ThT assay revealed no fibril formation even after the incubation time of 48 h. However, Helium-Air fed gas plasma for the treatment times of 8 and 10 min produced fibrils within 24 h. Figure 1 shows the ThT assay of both 8 and 10 min treated lysozyme, and the fibrillation dynamics shows the formation of the fibrils. The fibril formation is enhanced with respect to time, and we found the maximum after 24 h of incubation time. It can be noted that the fibrils formed using reported protocols[16,34] start initiating after 48−72 h and that with CAP treatment fibrils formation is initiated from 3 h and has a significant change after 24 h. The plasma is comprised of many reactive oxygen species/reactive nitrogen species (ROS/RNS), and their interaction with the protein triggers the fibril formation, which is similar to the case of neurodegeneration. For all the further studies, we treated the Lyz for 8 and 10 min under He-air feed gas plasma and incubated for 24 h at room temperature to form fibrils. These fibrils were further analyzed after interaction with the Keggin POMs.

CAP imparts ROS/RNS to the samples, which were measured using various assays as described in the Experimental Methods section. The quantification of the different ROS/RNS radicals is given in Table 1. It can be noted that the hydroxyl radicals produced during the CAP treatment are maximum for the 8 min treatment time, whereas the hydrogen peroxide radicals are maximum for the 10 min treatment time. This could be due to the conversion of the unstable hydroxyl radicals to the stable hydrogen peroxide radicals due to the increased treatment time due to CAP. The nitrate and nitrite ions are higher for 10 min of plasma treatment. The interactions of these ROS/RNS radicals with the protein could have led to the formation of fibrils as seen in the ThT assay.

The next part of the work was focused on the interaction of the fibrillated protein with the POMs. Figure 2 presents the common structure of the Keggin type POMs used in this study, and the two systems used were Phosphomolybdic acid (PMA)with the chemical formula $H_3[Mo_{12}PO_{40}]\cdot 12H_2O$.

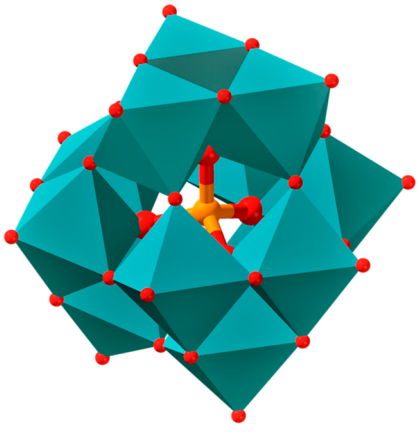

Figure 2. Common structure of the polyoxometalates used in this study.

https://doi.org/10.1021/acsomega.3c06921
ACS Omega 2024, 9, 3423−3429

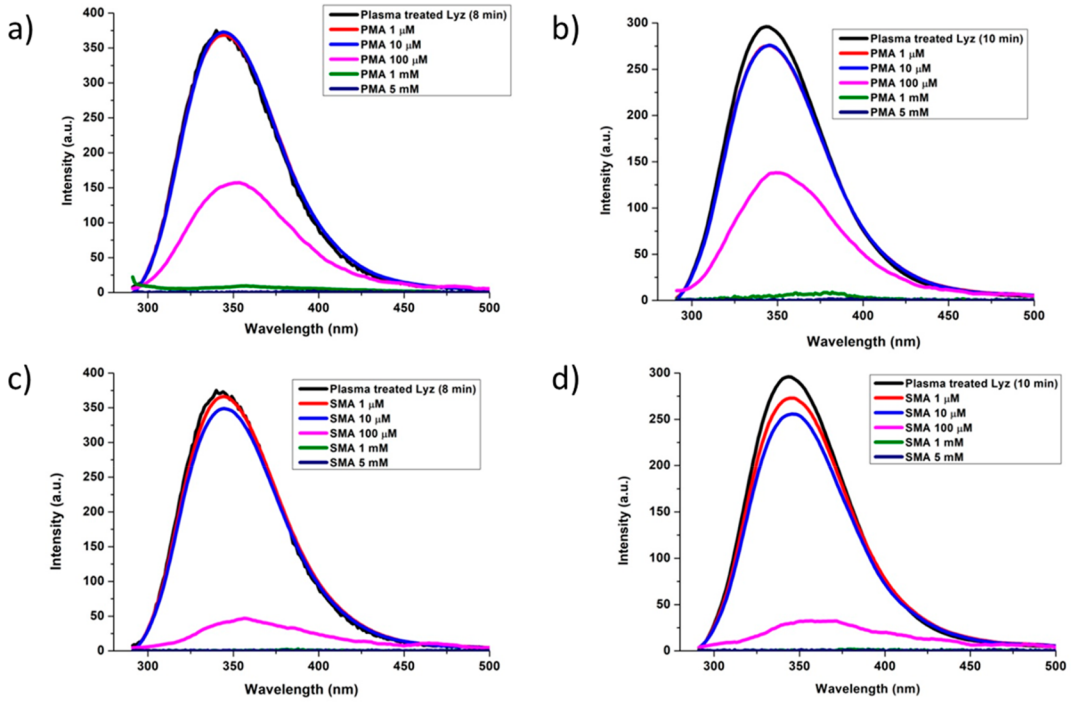

Figure 3. Fluorescence spectra of the Lyz fibrils after (a, c) 8 min treatment time and (b, d) 10 min treatment time with PMA/SMA.

and Silicomolybdic acid (SMA) with the chemical formula $SiO_2 \bullet 12MoO_3 \bullet xH_2O$. Both the POMS have a similar structure and are heteropolymetalates.

A preliminary study with different concentrations of the POMs was carried out to study the interaction with the lysozyme fibrils formed after 8 and 10 min of CAP treatment. Figure 3(a) and (b) show the interaction of PMA with the Lyz fibrils for the treatment times. Figure 3(c) and (d) show the interaction of SMA with Lyz fibrils. The PL spectra of the samples reveal a quenching of the fluorescence intensity with increase in concentration, and both POMs follow a similar trend, with SMA showing more pronounced quenching effect than PMA.

Interactions with the major residues in the protein Lyz were analyzed using molecular docking studies. Figure 4 presents the docking of PMA and SMA with Lyz (PDB ID: 1DPX). The docking studies show that the dominant hydrogen bonding interactions between POMs and the protein and especially in the Phe residue (Table 2) could be majorly responsible for the quenching of the fluorescence, as shown in Figure 3.

The major shift in the quenching of fluorescence as seen in Figure 3 could be due to the various charged interactions, and to assess the change in the surface charge the zeta potentials of the samples were measured. Table 3 presents the zeta potential of the Lyz fibrils (for the 10 min CAP treatment time) after interaction with the POMs. The control Lyz sample showed a zeta potential value of +1.48 mV, and gradually the value shifts to more negative values with the increase in the concentration of the PMA/SMA. This clearly suggests that the electrostatic interactions dominate the fibrils-POM interactions in addition to the hydrogen bonded interactions, as predicted by the docking studies.

ThT, a standard marker for evaluating β-sheets in the protein fibrils, shows an increased fluorescence upon binding to protein fibrils and aggregates. To further drive the analysis, the ThT assay (Figure 5) was carried out on the Lyz fibrils (10 min CAP treatment) after their interaction with PMA/SMA. Figure 5 shows that both PMA and SMA help in the reduction of the fibrils, as depicted by the low fluorescence intensity compared to the control; however, SMA has a more profound effect than PMA, with as low as10 μM concentration disrupting the fibrils and validating the zeta potential results. As discussed previously, the electrostatic and hydrogen bonded interactions have led to the binding of POMs to the fibrils and disruption of the fibrils.

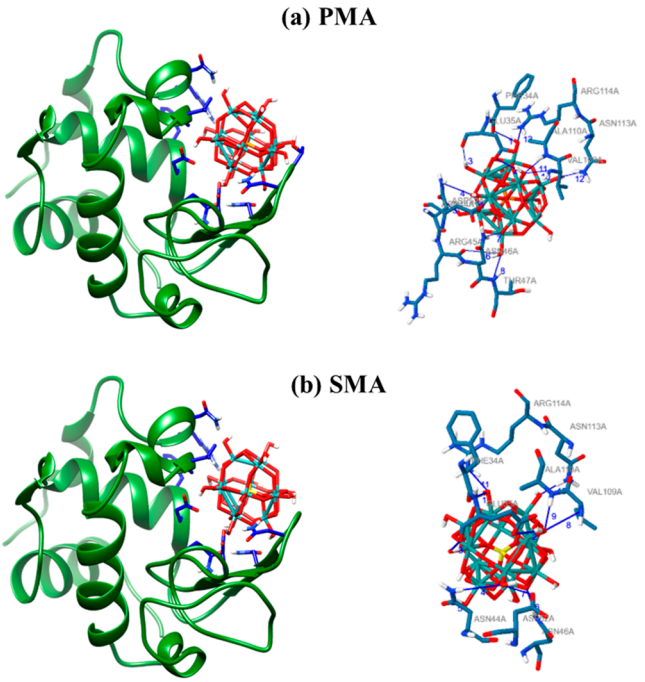

Figure 4. Molecular docking studies of Lyz with (a) PMA and (b) SMA.

https://doi.org/10.1021/acsomega.3c06921
ACS Omega 2024, 9, 3423−3429

Table 2. Binding Energy and Interacting Residues of Lys with PMA and SMA

S. no	Ligand	Binding energy (kcal/mol)	Interacting residues
1	PMA	−5.93	PHE_34, GLU_35, ASN_44, ARG_45, ASN_46, THR_47, ASP_52, VAL_109, ALA_110, ASN_113, ARG_114
2	SMA	−6.40	PHE_34, GLU_35, ASN_44, ASN_46, ASP_52, VAL_109, ALA_110, ASN_113, ARG_114

Table 3. Zeta Potential of Lyz Fibrils Treated with PMA/SMA

	Zeta Potential (mV)				
Sample	1 μM	10 μM	100 μM	1 mM	5 mM
Lyz Fibrils + PMA	0.46	−2.48	−18.15	−22.95	−25.75
Lyz Fibrils + SMA	0.54	−7.06	−21.3	−27.75	−26.3

The formation of Lyz fibrils and the disruption of the same with the POMs were further confirmed by TEM, as presented in Figure 6. For comparison, the Lyz monomer is presented in Figure 6(a) followed by the proteins treated for 8 min (Figure 6(b)) and 10 min (Figure 6(c)) under the Helium-Air CAP treatment. Figure 6(b) and Figure 6(c) together with the ThT analysis in Figure 5 strongly support the formation of fibril-like aggregate structures. This could be due to the presence of RONS in the CAP further driving the aggregation process, and such protein assemblies have been earlier reported by our group.[35] Further, Keggin POMs were added to the protein treated with CAP for 10 min (Figure 6(c)) and are presented for PMA in Figure 6(d) and for SMA in Figure 6(e). We clearly observe with TEM the disruption of the fibril-like aggregates upon POMs addition, as suggested by the observed significant shrinkage of the thick aggregates into thin fibrils and amorphous aggregates, which also validates the ThT assay. Such disruption of the amyloid aggregation using different POMs is reported.[36]

Enzyme activity plays a significant role in metabolism. In this work, we studied the activity of the Lyz fibrils after the addition of POMs as described in the Experimental Section. In general, prisitine Lyz reacts with the *Micrococcus lysodeikticus* (ATCC No. 4698, lyophilized cells (M3770)) cell wall suspension leading to the breakage of the bonds in the cell wall with a marked increase of the OD at 450 nm, indicating the measure of the interaction.[37] Hence, to ascertain the POMs' role after addition with the Lyz fibrils and its influence over the activity of the enzyme, the control/fibril samples were treated with the

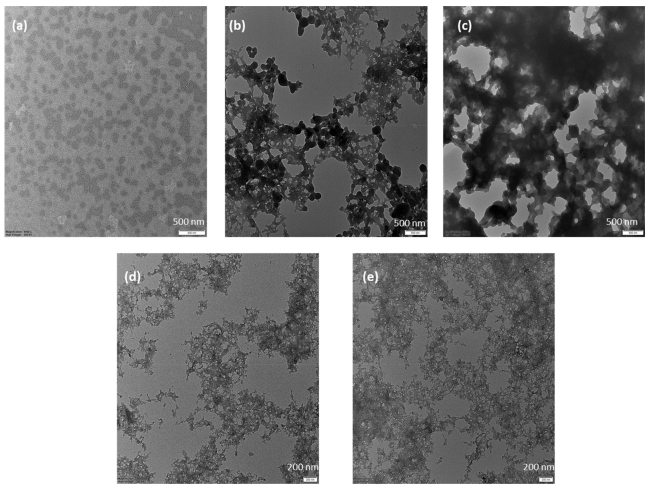

Figure 6. TEM images of the (a) lysozyme monomer; (b and c) lysozyme fibrils formed after (b) 8 min CAP treatment and (c) 10 min CAP treatment; (d) fibrils inhibited by PMA; and (e) fibrils inhibited by SMA.

Micrococcus lysodeikticus cell wall suspension post treatment with the POMs (Figure 7). We observe a drastic improvement in the activity of the Lyz with both the POMs; especially SMA has a higher capacity to regenerate the activity of the Lyz compared to PMA. Hence, it can be concluded that the POMs play a crucial role in improving the fibrillar activity of Lyz protein through various electrostatic interactions and further aid in regaining the activity.

4. CONCLUSIONS

We have studied two Keggin POMs, namely PMA and SMA, for their ability to interact with the neurodegenerative model protein Lyz. A special technique involving cold atmospheric pressure plasma was used to mimic the RONS generation leading to protein Lyz aggregation to fibrils. The fibrils were further treated with the POMs, and we observed the disruption of the fibrils using the ThT assay and TEM analysis to oligomer-like aggregates. Docking studies and zeta potential analysis showed that the disruption of the fibrils is driven by electrostatic and hydrogen bonding interactions. The activity of the protein after treatment with the POMs was measured, and the protein showed a drastic improvement in the activity with SMA compared to PMA. The results suggest that the Keggin POMs could possibly be used in therapeutic treatment of neurodegenerative disorders.

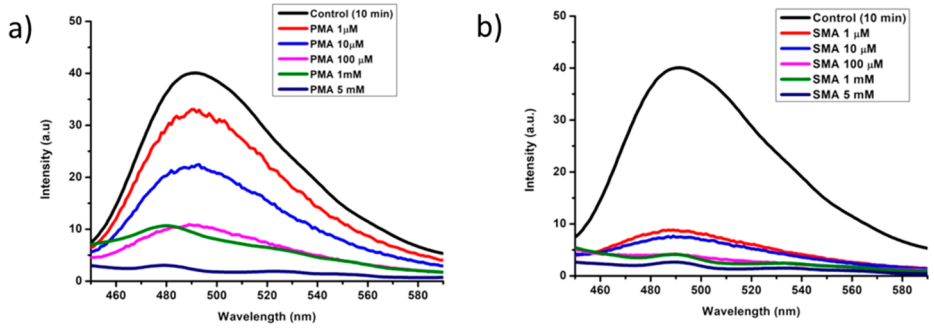

Figure 5. ThT assay of the fibrils' disruption using (a) PMA and (b) SMA.

https://doi.org/10.1021/acsomega.3c06921
ACS Omega 2024, 9, 3423−3429

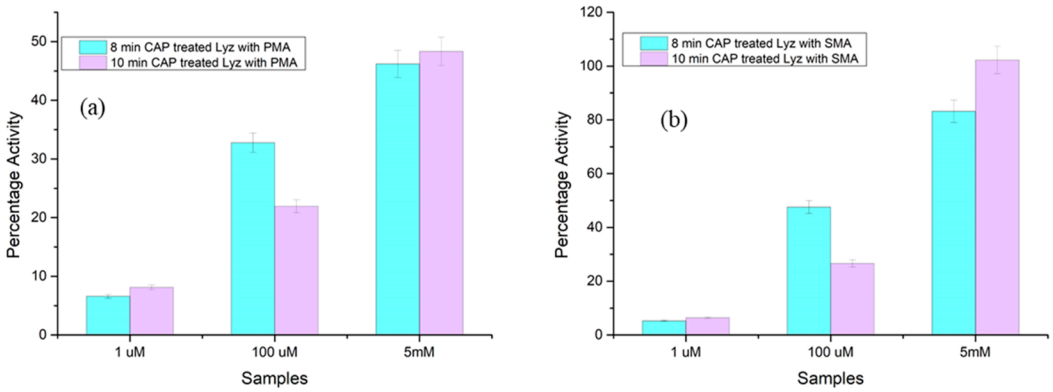

Figure 7. Percentage activity of the lysozyme fibrils with the *Micrococcus lysodeikticus* cell wall suspension after addition of (a) PMA and (b) SMA.

AUTHOR INFORMATION

Corresponding Author

Kamatchi Sankaranarayanan − *Physical Sciences Division, Institute of Advanced Study in Science and Technology (An Autonomous Institute Under DST, Government of India), Guwahati, Assam 781035, India;* orcid.org/0000-0002-2742-1994; Email: kamatchi.sankaran@gmail.com

Authors

Kaberi Kalita − *Physical Sciences Division, Institute of Advanced Study in Science and Technology (An Autonomous Institute Under DST, Government of India), Guwahati, Assam 781035, India*

Shankab J. Phukan − *Department of Chemistry, Institute of Science, Banaras Hindu University, Varanasi 221005 Uttar Pradesh, India*

Somenath Garai − *Department of Chemistry, Institute of Science, Banaras Hindu University, Varanasi 221005 Uttar Pradesh, India*

Complete contact information is available at: https://pubs.acs.org/10.1021/acsomega.3c06921

Notes

The authors declare no competing financial interest.

ACKNOWLEDGMENTS

K.S. thanks SERB, Govt. of India for the SRG grant (SRG/2020/001894 dt. 11.11.2020), and DST-IASST, Guwahati, for the in-house project grant. S.G. thanks SERB, SPARC, DST, and BHU-IoE for financial support. K.S. thanks Mounish Reddy for help with the docking studies.

REFERENCES

(1) Banerjee, R. Effect of Curcumin on the metal ion induced fibrillization of Amyloid-β peptide. *Spectrochim Acta A Mol. Biomol Spectrosc* **2014**, *117*, 798−800.

(2) Wang, Q.; Yu, X.; Li, L.; Zheng, J. Inhibition of Amyloid-β Aggregation in Alzheimer's Disease. *Curr. Pharm. Design* **2014**, *20*, 1223−1243.

(3) Okuno, H.; Mori, K.; Okada, T.; Yokoyama, Y.; Suzuki, H. Development of aggregation inhibitors for amyloid-β peptides and their evaluation by quartz-crystal microbalance. *Chem. Biol. Drug Des.* **2007**, *69*, 356−361.

(4) Estrada, L. D.; Soto, C. Disrupting β-Amyloid Aggregation for Alzheimer Disease Treatment. *Curr. Top. Med. Chem.* **2007**, *7*, 115−126.

(5) Morgado, I.; Fändrich, M. Assembly of Alzheimer's Aβ peptide into nanostructured amyloid fibrils. *Curr. Opin. Colloid Interface Sci.* **2011**, *16*, 508−514.

(6) Cheignon, C.; Tomas, M.; Bonnefont-Rousselot, D.; Faller, P.; Hureau, C.; Collin, F. Oxidative stress and the amyloid beta peptide in Alzheimer's disease. *Redox Biol.* **2018**, *14*, 450−464.

(7) Hu, W. P.; Chang, G. L.; Chen, S. J.; Kuo, Y. M. Kinetic analysis of β-amyloid peptide aggregation induced by metal ions based on surface plasmon resonance biosensing. *J. Neurosci. Methods,* **2006**, *154*, 190−197.

(8) Tõugu, V.; Tiiman, A.; Palumaa, P. Interactions of Zn(II) and Cu(II) ions with Alzheimer's amyloid-beta peptide. Metal ion binding, contribution to fibrillization and toxicity. *Metallomics* **2011**, *3*, 250−261.

(9) Qiang, W.; Yau, W. M.; Schulte, J. Fibrillation of β amyloid peptides in the presence of phospholipid bilayers and the consequent membrane disruption. *Biochim. Biophys. Acta, Biomembr.* **2015**, *1848*, 266−276.

(10) Han, X.; He, G. Toward a Rational Design to Regulate β-Amyloid Fibrillation for Alzheimer's Disease Treatment. *ACS Chem. Neurosci.* **2018**, *9*, 198−210.

(11) Patel, P.; Parmar, K.; Patel, D.; Kumar, S.; Trivedi, M.; Das, M. Inhibition of amyloid fibril formation of lysozyme by ascorbic acid and a probable mechanism of action. *Int. J. Biol. Macromol.* **2018**, *114*, 666−678.

(12) Ow, S. Y.; Dunstan, D. E. A brief overview of amyloids and Alzheimer's disease. *Protein Sci.* **2014**, *23*, 1315−1331.

(13) Chiti, F.; Dobson, C. M. Protein misfolding, functional amyloid, and human disease. *Annu. Rev. Biochem.* **2006**, *75*, 333−366.

(14) Arnaudov, L. N.; de Vries, R. Thermally Induced Fibrillar Aggregation of Hen Egg White Lysozyme. *Biophys. J.* **2005**, *88*, 515−526.

(15) Perez, C.; Miti, T.; Hasecke, F.; Meisl, G.; Hoyer, W.; Muschol, M.; Ullah, G. Mechanism of Fibril and Soluble Oligomer Formation in Amyloid Beta and Hen Egg White Lysozyme Protein. *J. Phys. Chem. B* **2019**, *123*, 5678−5689.

(16) Cao, A.; Hu, D.; Lai, L. Formation of amyloid fibrils from fully reduced hen egg white lysozyme. *Protein Sci.* **2004**, *13*, 319−324.

(17) Laroussi, M. Cold Plasma in Medicine and Healthcare: The New Frontier in Low Temperature Plasma Applications. *Front. Phys.* **2020**, *8*, 74.

(18) Choi, S.; Attri, P.; Lee, I.; Oh, J.; Yun, J. H.; Park, J. H.; Choi, E. H.; Lee, W. Structural and functional analysis of lysozyme after treatment with dielectric barrier discharge plasma and atmospheric pressure plasma jet. *Sci. Rep.* **2017**, *7*, 1027.

(19) Martínez-Ojeda, R. M.; Pérez-Cárceles, M. D.; Ardelean, L. C.; Stanciu, S. G.; Bueno, J. M. Multiphoton microscopy of oral tissues. *Front. Phys.* **2020**, *8*, 128.

(20) Bernard, C.; Leduc, A.; Barbeau, J.; Saoudi, B.; Yahia, L'H.; De Crescenzo, G. Validation of cold plasma treatment for protein

https://doi.org/10.1021/acsomega.3c06921
ACS Omega 2024, 9, 3423−3429

inactivation: a surface plasmon resonance-based biosensor study. *J. Phys. D: Appl. Phys.* **2006**, *39*, 3470.
(21) Ji, H.; Han, F.; Peng, S.; Yu, J.; Li, L.; Liu, Y.; Chen, Y.; Li, S.; Chen, Y. Behavioral solubilization of peanut protein isolate by atmospheric pressure cold plasma (ACP) treatment. *Food Bioprocess Technol.* **2019**, *12*, 2018−2027.
(22) Pope, M. T. Polyoxometalates. In *Encyclopedia of Inorganic and Bioinorganic Chemistry*; Scott, R. A., Ed.; Wiley, 2005 DOI: 10.1002/9781119951438.eibc0185.
(23) Hasenknopf, B. Polyoxometalates: introduction to a class of inorganic compounds and their biomedical applications. *Front. Biosci.* **2005**, *10*, 275−287.
(24) Geng, J.; Li, M.; Ren, J.; Wang, E.; Qu, X. Polyoxometalates as inhibitors of the aggregation of amyloid β peptides associated with Alzheimer's disease. *Angew. Chem., Int. Ed.* **2011**, *50*, 4184−4188.
(25) Van Rompuy, L. S.; Parac-Vogt, T. N. Interactions between polyoxometalates and biological systems: From drug design to artificial enzymes. *Curr. Opin. Biotechnol.* **2019**, *58*, 92−99.
(26) Lee, B. I.; Chung, Y. J.; Park, C. B. Photosensitizing materials and platforms for light-triggered modulation of Alzheimer's β-amyloid self-assembly. *Biomaterials* **2019**, *190*, 121−132.
(27) Chen, Q.; Yang, L.; Zheng, C.; Zheng, W.; Zhang, J.; Zhou, Y.; Liu, J. Mo polyoxometalate nanoclusters capable of inhibiting the aggregation of Aβ-peptide associated with Alzheimer's disease. *Nanoscale* **2014**, *6*, 6886−6897.
(28) Gao, N.; Dong, K.; Zhao, A.; Sun, H.; Wang, Y.; Ren, J.; Qu, X. Polyoxometalate-based nanozyme: design of a multifunctional enzyme for multi-faceted treatment of Alzheimer's disease. *Nano Research* **2016**, *9*, 1079−1090.
(29) Sandhir, R.; Yadav, A.; Sunkaria, A.; Singhal, N. Nano-antioxidants: an emerging strategy for intervention against neuro-degenerative conditions. *Neurochem. Int.* **2015**, *89*, 209−226.
(30) Khanikar, R. R.; Kalita, M.; Kalita, P.; Kashyap, B.; Das, S.; Khan, M. R.; Bailung, H.; Sankaranarayanan, K. Cold atmospheric pressure plasma for attenuation of SARS-CoV-2 spike protein binding to ACE2 protein and the RNA deactivation. *RSC Adv.* **2022**, *12*, 9466−9472.
(31) Adasme, M. F.; Linnemann, K. L.; Bolz, S. N.; Kaiser, F.; Salentin, S.; Haupt, V. J.; Schroeder, M. PLIP 2021: Expanding the scope of the protein−ligand interaction profiler to DNA and RNA. *Nucleic Acids Res.* **2021**, *49*, W530−W534.
(32) Dallakyan, S.; Olson, A. J. Small-molecule library screening by docking with PyRx. *Chemical Biology: Methods and Protocols* **2015**, *1263*, 243.
(33) Morris, G. M.; Huey, R.; Lindstrom, W.; Sanner, M. F.; Belew, R. K.; Goodsell, D. S.; Olson, A. J. AutoDock4 and AutoDockTools4: Automated docking with selective receptor flexibility. *J. Comput. Chem.* **2009**, *30*, 2785−2791.
(34) Humblet-Hua, N. P.; Sagis, L. M.; van der Linden, E. Effects of flow on hen egg white lysozyme (HEWL) fibril formation: length distribution, flexibility, and kinetics. *J. Agric. Food Chem.* **2008**, *56*, 11875−11882.
(35) Bharati, A. J.; Khanikar, R. R.; Bailung, H.; Sankaranarayanan, K. Investigating the effect of atmospheric plasma on protein fibrinogen: Spectroscopic and biophysical analysis. *Plasma Processes Polym.* **2023**, 2300127.
(36) Chaudhary, H.; Iashchishyn, I. A.; Romanova, N. V.; Rambaran, M. A.; Musteikyte, G.; Smirnovas, V.; Holmboe, M.; Ohlin, C. A.; Svedružić, Z. M.; Morozova-Roche, L. A. Polyoxometalates as effective nano-inhibitors of amyloid aggregation of pro-inflammatory S100A9 protein involved in neurodegenerative diseases. *ACS Appl. Mater. Interfaces* **2021**, *13*, 26721−26734.
(37) Prager, E. M.; Arnheim, N.; Mross, G. A.; Wilson, A. C. Amino acid sequence studies on bobwhite quail egg white lysozyme. *J. Biol. Chem.* **1972**, *247*, 2905−2916.

https://doi.org/10.1021/acsomega.3c06921
ACS Omega 2024, 9, 3423−3429